Preprint. To appear in *Proceedings of the 29th International Symposium on Shock Waves*, Madison, WI, July 2013. Springer.

Final version will be available from Springer.

Shock tunnel operation and correlation of boundary layer transition on a cone in hypervelocity flow

J.S. Jewell[1], **J.E. Shepherd**[1], **and I.A. Leyva**[2]

1 Introduction

The Caltech T5 reflected shock tunnel is used to produce hypervelocity flow over a range of velocities and pressures by varying the test gas and operating parameters of reservoir enthalpy (h_{res}) and reservoir pressure (P_{res}). One area of research in T5 is the measurement of boundary layer behavior and transition from laminar to turbulent flow on a smooth 5-degree half-angle cone [3, 1, 11]. To design experiments that involve the measurement or manipulation of instability and transition processes (for example, Jewell et al. [7]), it is important to choose tunnel conditions for which the expected transition location is at least approximately known. In the present paper, we discuss the selection of tunnel operating parameters, the correlation of those parameters with measurements of boundary layer transition, and some observations on the analysis of transition location in terms of local boundary layer properties.

2 Tunnel Operation

Flow conditions in T5 are calculated from three tunnel measurements: the shock speed, initial shock tube fill pressure and composition, and reservoir pressure at the end of the shock tube during the run time [4]. Only experiments with measured shock speeds that fall within the uncertainty for the adjusted shock speed curve predicted by the shock jump conditions from the primary diaphragm burst pressure, driver gas composition, and initial shock tube conditions are included in the present data set.

There are a number of other potential sources of measurement error, bias, or uncertainties. These include: nonideal gas behavior in the reservoir due to the high

California Institute of Technology, 1200 E. California Blvd., Pasadena, CA 91125, USA · Air Force Research Laboratory, 4 Draco Dr., Edwards AFB, CA 93524, USA

pressure; the extrapolation of the shock speed (which decays as it propagates down the shock tube) to the end wall; nonuniformity of reservoir conditions due to non-ideal shock reflection; and the method of correcting flow conditions from the ideal reflected-shock pressure to measured reservoir pressure using an isentropic expansion. Furthermore, the 1-D nozzle computation does not account for boundary layer growth within the nozzle, off-design operation conditions that lead to flow nonuniformity, or vibration-translation nonequilibrium and freezing within the nozzle, which is significant for the N_2 cases. For the uncertainties that can be quantified, we have combined these to obtain the error bounds on measured properties that are shown in this paper. The tunnel parameters for the present studies in air and nitrogen

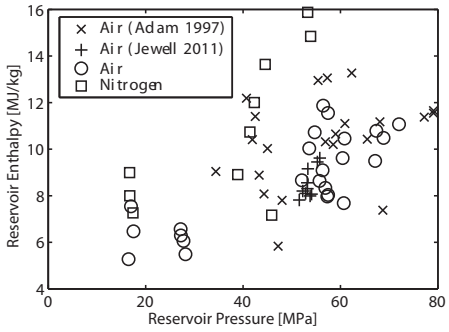

Fig. 1 Tunnel operating parameters h_{res} and P_{res} for the present studies in air and N_2, compared with past results from Adam [1] and Jewell et al. [5].

are compared with those of two past data sets in air in Figure 1. The present work both overlaps and extends the parameters of the past studies, especially for low pressure and enthalpy. The R^2 values for the correlation between the two parameters are respectively 0.52 and 0.65 for the present N_2 and Air data sets, and respectively 0.10 and 0.59 for the Adam [1] and Jewell et al. [5] data sets.

Freestream conditions are taken as the conditions at the nozzle exit. The 100:1 area ratio contoured nozzle is designed to operate at Mach 6. Because the shape is optimized for a single condition, there is significant variation of the exit Mach number over the range of tunnel operating parameters, presented in Figure 2 for air over the conditions of the present study.

3 Experiments

The experimental model is a 1-m long, smooth, 5-degree half-angle cone with a nominally sharp tip of radius 0.18 mm and oriented at a zero angle of attack. The range of Reynolds numbers evaluated at the boundary layer edge and Dorrance [2] reference temperature, which is used as representative of conditions within the

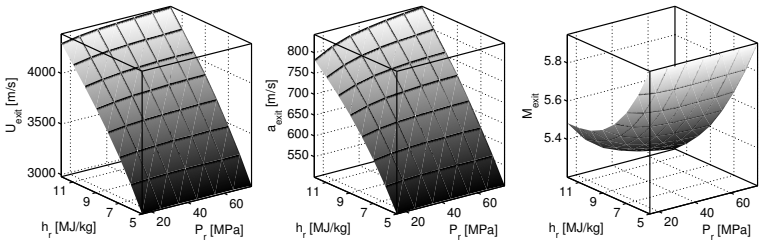

Fig. 2 Calculated nozzle exit velocity, sound speed, and Mach number in air over a range of tunnel operating parameters h_{res} and P_{res}.

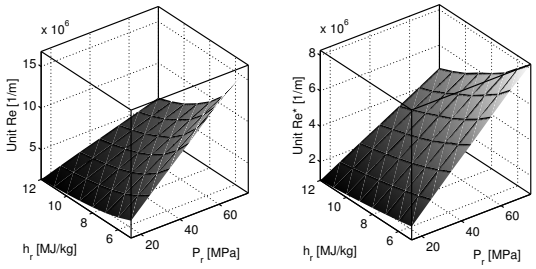

Fig. 3 Reynolds number evaluated at the boundary layer edge in air (left) and at Dorrance reference conditions in air (right) over a range of tunnel operating parameters h_{res} and P_{res}.

boundary layer, is presented for air in Figure 3. The cone is instrumented with 80 thermocouples, providing heat transfer measurements from which transition location may be determined. Heat transfer results are normalized by Stanton number and Reynolds number, and the location of transition onset determined as described in Jewell et al. [7].

Parameters for experiments that bracket the range of conditions studied in both air and N_2 are presented in Table 1. A supplemental report [6] is available online, which includes the full tables and plots for all 34 experiments included in the present study.

4 Results and Analysis

Results for the location X_{tr} of transition onset on the cone are presented in terms of h_{res} and P_{res} in Figure 4 for both N_2 and air. Multivariable linear regression analysis is performed on these data sets (for details, see [6]). Both the present N_2 and air results have a positive dependence on h_{res} (linear model coefficient of 0.56 for N_2, 0.55 for air) and a negative dependence on P_{res} (linear model coefficient of -0.45 for N_2, -0.15 for air). The historical air data of Adam and Hornung[1], are analyzed in the same way, and likewise show a significant positive dependence of X_{tr} on h_{res}

Table 1 Parameters for selected experiments spanning the present range of conditions for air and N_2.

	Gas	h_{res} [MJ/kg]	P_{res} [MPa]	Re$/m$ [1/m]	Re$^*/m$ [1/m]	X_{tr} [m]	δ_{99tr} [mm]	f_{tr} [kHz]
2744	Air	7.68	60.7	8.19×10^6	5.39×10^6	0.51	0.98	1094
2758	Air	11.07	72.0	6.11×10^6	4.79×10^6	0.74	1.26	1002
2764	Air	5.27	16.5	3.62×10^6	1.83×10^6	0.52	1.65	551
2773	N_2	8.99	16.7	2.02×10^6	1.25×10^6	0.67	2.26	522
2776	N_2	7.17	45.9	7.09×10^6	3.94×10^6	0.39	0.97	1102
2783	N_2	15.88	53.3	3.20×10^6	2.62×10^6	0.63	1.56	966

(linear model coefficient of 0.72) and negative dependence on P_{res} (linear model coefficient of -0.28).

Both the present N_2 and air results have a positive dependence on P_{res} (linear model coefficients of 0.31 for N_2, 0.59 for air) for the transition Reynolds number evaluated at Dorrance reference conditions, Re^*_{tr}, but neither have a dependence on h_{res} that is statistically significant. The historical air data of Adam and Hornung[1] likewise show a significant positive dependence of Re^*_{tr} on P_{res} (linear model coefficient of 0.34), but no statistically significant dependence on h_{res}.

The usual approach [12] for representing boundary layer transition onset is in terms of a transition location Reynolds number Re_{tr} or Re^*_{tr} and previous analysis [1] of T5 data has utilized this approach. However, in hypervelocity flow with a cold wall, the principal boundary layer instability mechanism is the predominantly inviscid acoustic or Mack mode [9]. Unlike the viscous instability of low-speed boundary layers, at high speeds the role of viscosity is primarily in determining the mean flow. The properties of the acoustic instability are determined by the local boundary layer thickness and profiles of velocity and thermodynamic properties. This suggests the approach of correlating transition distance with $X_{tr}/\delta_{.99}$ and the acoustic properties of the boundary layer rather than a Reynolds number.

As shown in Figure 5(l), $X_{tr}/\delta_{.99}$ is relatively independent of edge Mach number but shows a systematic dependence on the gas type and pressure. The scaled distance ranges from about 300 for low pressure tests up to 600 for high pressure. The radiation of acoustic disturbances from the turbulent boundary layer on the nozzle wall and the jet shear layer is an important source of disturbances in ground-testing facilities [12], and varying receptivity of the boundary layer to these radiated disturbances is a likely explanation for the trends observed in Figure 5.

Lowering the pressure creates a thicker boundary layer, and therefore lowers the most amplified second mode frequency $f \approx 0.6U_e/2\delta_{.99}$. This may account for the striking correlation of $X_{tr}/\delta_{.99}$ with the frequency f_{tr} that is shown in Figure 5(r). The influence on transition location can be explained by the measurements of Parziale et al. [10], who showed that in T5, most of the noise in the free stream is at relatively low frequencies (< 500 kHz), and observed a decrease in rms density fluctuations with increasing frequency. This is consistent with the present observa-

tions of earlier transition, at lower most-amplified frequencies, for lower values of P_{res} in both air and N_2.

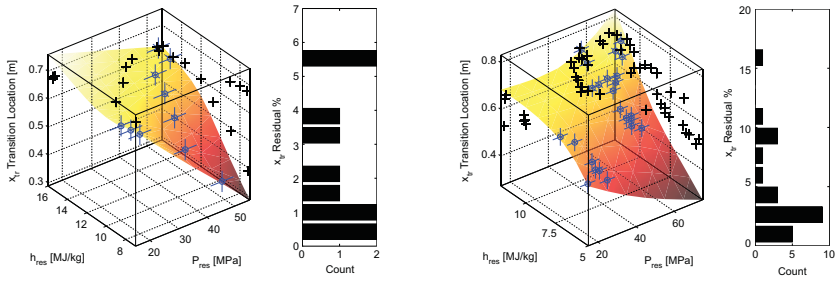

Fig. 4 (l) Transition onset location X_{tr} for N_2, and (r) air in terms of reservoir enthalpy h_{res} and pressure P_{res}.

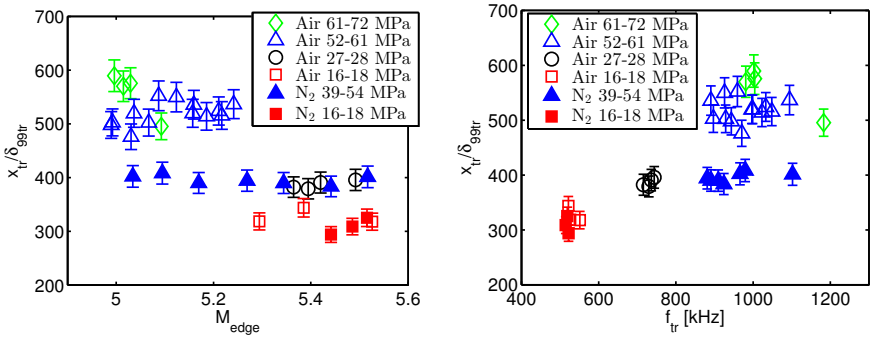

Fig. 5 (l) Scaled transition distance $X_{tr}/\delta_{.99tr}$ vs. M_{edge}, the boundary layer edge Mach number. (r) Scaled transition distance $X_{tr}/\delta_{.99tr}$ vs. f_{tr}, the approximate most-amplified second mode frequency at transition.

5 Conclusion

We have re-examined the correlation of transition onset data with tunnel operating conditions by modeling transition onset location with two-dimensional response surfaces in terms of h_{res} and P_{res} variables. We observe a positive correlation of X_{tr} with h_{res} in both air and N_2 and a negative correlation of X_{tr} with P_{res}. The parameter Re^*_{tr} exhibits a positive correlation with reservoir pressure in both gases. Controlling for variations in P_{res}, no statistically significant dependence of Re^*_{tr} on h_{res} was found for either the present air or N_2 data or the historical air data in Adam

and Hornung[1]. We explore an alternative normalization of the transition onset location by the local laminar boundary layer thickness $X_{tr}/\delta_{.99}$ and find that this is essentially independent of the edge Mach number for a given gas type and pressure range (Figure 5). We examine the correlation of transition onset with the most amplified acoustic frequency in the boundary layer and find that lower frequencies correlate with smaller values of normalized transition distance $X_{tr}/\delta_{.99}$, suggesting that the frequency-dependent amplification of the tunnel noise may be responsible for the observed systematic variations in transition onset distance.

Acknowledgements: The authors thank the T5 group members: Prof. Hans Hornung, Mr. Nick Parziale, and Mr. Bahram Valiferdowsi; Dr. Ross Wagnild for substantial assistance with the flow and boundary layer analysis; and Miss Elizabeth Jewell for her statistical advice. This project was sponsored by the Air Force Office of Scientific Research under award number FA9550-10-1-0491 (J. Schmisseur, program manager). The views expressed herein are those of the authors and should not be interpreted as necessarily representing the official policies or endorsements, either expressed or implied, of AFOSR or the U.S. Government.

References

1. Adam P.H. and Hornung H.G. (1997) Enthalpy Effects on Hypervelocity Boundary-Layer Transition: Ground Test and Flight Data. Journal of Spacecraft and Rockets, Vol. 34, No. 5, pp. 614–619.
2. Dorrance W.H. (1962) *Viscous Hypersonic Flow: Theory of Reacting and Hypersonic Boundary Layers*. McGraw-Hill.
3. Germain P. and Hornung H.G. (1997) Transition on a Slender Cone in Hypervelocity Flow. Experiments in Fluids, Vol. 22, pp. 183–190.
4. Hornung H.G. (1992) Performance data of the new free-piston shock tunnel at GALCIT. AIAA 92-3943.
5. Jewell J.S., Leyva I.A., Parziale N.J. and Shepherd J.E. (2011) Effect of gas injection on transition in hypervelocity boundary layers. *Proceedings of the 28th International Symposium on Shock Waves*, Vol. 1, pp. 735–740.
6. Jewell J.S., Shepherd J.E., and Leyva I.A. (2013) Supplemental data for "Shock tunnel operation and correlation of boundary layer transition" Available at http://www2.galcit.caltech.edu/T5/publications/publications.html
7. Jewell J.S., Wagnild R.M., Leyva I.A., Candler G.V. and Shepherd J.E. (2013) Transition within a hypervelocity boundary layer on a 5-degree half-angle cone in air/CO_2 mixtures. AIAA 2013-0523.
8. Leyva I.A., Jewell J.S., Laurence S., Hornung H.G. and Shepherd J.E. (2009) On the impact of injection schemes on transition in hypersonic boundary layers. AIAA 2009-7204.
9. Mack L.M. (1984) Boundary-layer stability theory. *Special Course on Stability and Transition of Laminar Flow*. AGARD Report 709.
10. Parziale N.J., Shepherd J.E. and Hornung H.G. (2012) Reflected shock tunnel noise measurement by focused differential interferometry. AIAA 2012-3261.
11. Rasheed A., Hornung H.G., Fedorov A.V. and Malmuth N.D. (2002) Experiments on Passive Hypervelocity Boundary-Layer Control Using an Ultrasonically Absorptive Surface. AIAA Journal, Vol. 40, No. 3.
12. Schneider S.P (2001) Effects of High-Speed Tunnel Noise on Laminar-Turbulent Transition. Journal of Spacecraft and Rockets, Vol. 38, No. 3, pp. 323–333.